Characterizing a transition from limited to unlimited diffusion in energy for a time-dependent stochastic billiard

Felipe Augusto O. Silveira,[1,2] Anne Kétri P. da Fonseca,[1] Peter Schmelcher,[2,3]
Denis G. Ladeira,[4] and Edson D. Leonel[1]
[1]Departamento de Física, UNESP – Universidade Estadual Paulista, Avenida 24A, 1515, Bela Vista, CEP 13506-900, Rio Claro, São Paulo, Brazil
[2]Zentrum für Optische Quantentechnologien, Universität Hamburg, Luruper Chaussee 149, 22761 Hamburg, Germany
[3]The Hamburg Centre for Ultrafast Imaging, Universität Hamburg, Luruper Chaussee 149, 22761 Hamburg, Germany
[4]Departamento de Estatística, Física e Matemática, UFSJ – Universidade Federal de São João del-Rei, Rodovia MG 443, Km 7, Fazenda do Cadete, CEP 36420-000, Ouro Branco, Minas Gerais, Brazil

(Received 11 November 2022; revised 28 July 2023; accepted 26 September 2023; published 6 November 2023)

We explore Fermi acceleration in a stochastic oval billiard which shows unlimited to limited diffusion in energy when passing from the free to the dissipative case. We provide evidence for a transition from limited to unlimited energy growth taking place while detuning the corresponding restitution coefficient responsible for the degree of dissipation. A corresponding order parameter is suggested, and its susceptibility is shown to diverge at the critical point. We show that this order parameter is also be applicable to the periodically driven oval billiard and discuss the elementary excitation of the controlled diffusion process.

DOI: 10.1103/PhysRevE.108.054206

I. INTRODUCTION

Billiards represent dynamical systems composed of particles moving inside a closed boundary while colliding with the latter [1,2]. Generally, the border may assume many geometrical shapes and can even depend on time. It is well known that a phenomenon denoted as Fermi acceleration (FA) is observed for time-dependent boundaries. In the case of FA, an ensemble of particles acquires, on average, unlimited energy growth from collisions with the border. The Loskutov-Ryabov-Akinshin (LRA) conjecture [3,4] states that chaos in a static billiard is a sufficient condition to observe FA when a time-dependent perturbation to the boundary is introduced.

Examples of time-dependent billiards exhibiting FA include the Lorentz gas [5,6], the stadium billiard [7], and the oval billiard [8]. A well-known example complementing the LRA conjecture is the elliptical billiard [9]. The static version of the elliptical billiard is integrable. When a time perturbation to the boundary is introduced, depending on the initial condition as well as the control parameters, FA is observed. Due to the boundary's time variation, the separatrix present in the phase space is replaced by a stochastic layer. Therefore, trajectories confined inside the separatrix (librators) can explore regions outside the separatrix (rotators) and vice versa. These crossings define a mechanism producing the unlimited energy growth [9,10]. It has been noticed that FA is not robust under inelastic collisions [11] since even for the smallest amount of dissipation, FA is suppressed. For the dissipative billiard, the appearance of attractors leads the mean velocity to enter a saturation regime for large enough times, and the energy gain of the particles becomes limited [12].

The phenomena of Fermi acceleration and its suppression have also been observed in the context of stochastic billiards [13,14]. In those systems, the stochasticity can be introduced through random reflections [15], random oscillations of the boundary [8], or even by turning dynamical variables into random variables with fixed in time probability distributions [16]. The main physical motivations for studying stochastic billiards come from the need to understand diffusive motion in porous media [17] and to create models for the exploration of stochastic processes such as Markov chains [18] and Brownian motion [19]. Moreover, stochastic nonlinear dynamical systems can be used to model chaotic systems in statistical physics, regardless of whether or not they are in equilibrium [20,21].

For many nonlinear systems, some physical observables obey properties linked to scale invariance that inevitably lead to scaling laws [22–27], which are commonly related to phase transitions [28,29]. Although scale invariance and power laws have been found in many different nonlinear dynamical systems, little is known about possible related phase transition. In statistical physics, phase transitions are often related to changes in the spatial structure of a system caused by the variation of control parameters [30,31]. Conversely, in dynamical systems, phase transitions are linked to changes in their phase space structure, also due to changes in the corresponding control parameters [32,33]. Close to a phase transition, the relevant observables obey a scaling behavior and exhibit critical exponents that characterize the system's dynamics.

In this paper, we study a transition from limited to unlimited energy growth (TLUG) in a stochastic oval billiard whose boundary moves in time. The particle, or in an equivalent way, an ensemble of noninteracting particles, collides with the moving boundary. The reflection law considers inelastic collisions that preserve the tangential momentum but not the kinetic energy upon collision. We assume only the normal component of the velocity to be affected by the dissipation, which is controlled by a restitution coefficient. The static oval billiard exhibits a mixed-phase space; therefore, the LRA conjecture applies. With an increasing number of collisions, the growth of the average velocity of the particles is unbounded, leading to the unlimited diffusion of energy. Dissipation occurs when the restitution coefficient is less than one, and unbounded energy growth is no longer observed. Hence the dynamics of the average velocity evolves to a stationary state, confirming the suppression of the unlimited energy growth. This suppression of unlimited growth marks the transition in which we are interested. When the dissipation parameter approaches one continuously, the average velocity saturation plateau increases indefinitely. The inverse of the saturation plateau approaches zero at this transition and, as we shall see, defines a candidate for an order parameter. At the critical point, the corresponding susceptibility diverges.

Moreover, we identify the elementary excitation of the dynamics, which is responsible for the chaotic diffusion in the phase space. We also discuss the applicability of the employed method to the time-driven oval billiard.

II. THE MODEL

The main goal of this paper is to characterize a transition from limited to unlimited energy gain for an ensemble of noninteracting particles confined within an stochastic oval billiard whose boundary oscillates in time. The equation of the border is given by

$$R(\theta, \varepsilon, \eta, t, p) = 1 + \varepsilon[1 + \eta\cos(t)]\cos(p\theta), \qquad (1)$$

where p is an integer, and ε is a parameter responsible for the geometrical deformation. For $\varepsilon = 0$, the billiard is a circle. The control parameter η determines the amplitude of the time perturbation of the boundary, and the case $\eta = 0$ recovers the static billiard. The dynamics of a particle is specified in terms of its velocity V_n, the angular position θ_n, the angle α_n that its trajectory forms with a tangent line at the position of the collision, and the time of the collision t_n as

$$X(t) = X(\theta_n, t_n) + V_n\cos(\alpha_n + \phi_n)(t - t_n), \qquad (2)$$

$$Y(t) = Y(\theta_n, t_n) + V_n\sin(\alpha_n + \phi_n)(t - t_n), \qquad (3)$$

where the time $t \geqslant t_n$ with $X(\theta_n, t_n) = R(\theta_n, t_n)\cos(\theta_n)$ and $Y(\theta_n, t_n) = R(\theta_n, t_n)\sin(\theta_n)$. Once the angle θ is known, the angle ϕ is obtained and corresponds to the angle formed between the tangent and horizontal lines at the position $X(\theta), Y(\theta)$, which can be written as $\phi = \arctan[Y'(\theta, t)/X'(\theta, t)]$ where Y' and X' are derivatives with respect to θ. Figure 1 illustrates the billiard under investigation for $\varepsilon = 10^{-2}$, $\eta = 20$, and $p = 3$. The green and violet curves represent the boundary of the billiard at two instants. Figure 1(a) depicts a portion of the particle's trajectory. At instant t_n, the particle collides against the boundary and acquires velocity $\mathbf{V}_n$. The point of the nth collision is characterized by the polar coordinates (R_n, θ_n). After a time interval traveling in a straight line, the particle reaches the boundary at instant t_{n+1} and, immediately after the collision, its velocity is $\mathbf{V}_{n+1}$. The gray region represents the portion of space outside the time-dependent boundary. Figure 1(b) corresponds to an amplification of the top left portion of the billiard illustrated in Fig. 1(a), where the particle undergoes the nth collision. In this figure, we use dashed lines to represent the tangent and normal directions relative to the boundary at the instant of the nth collision. This figure also presents the variable α_n, which is the outgoing angle between the vector velocity and the line tangent to the boundary. We also include in Fig. 1(b) the components of $\mathbf{V}_n$ relative to the tangent and normal directions with blue color. Considering that the particle travels with constant speed between collisions, its position within the billiard is given in polar coordinates as $R_p(t) = \sqrt{X^2(t) + Y^2(t)}$. The angular position θ at the instant of impact is found numerically through the equation $R_p(\theta_{n+1}, t_{n+1}) = R(\theta_{n+1}, t_{n+1})$.

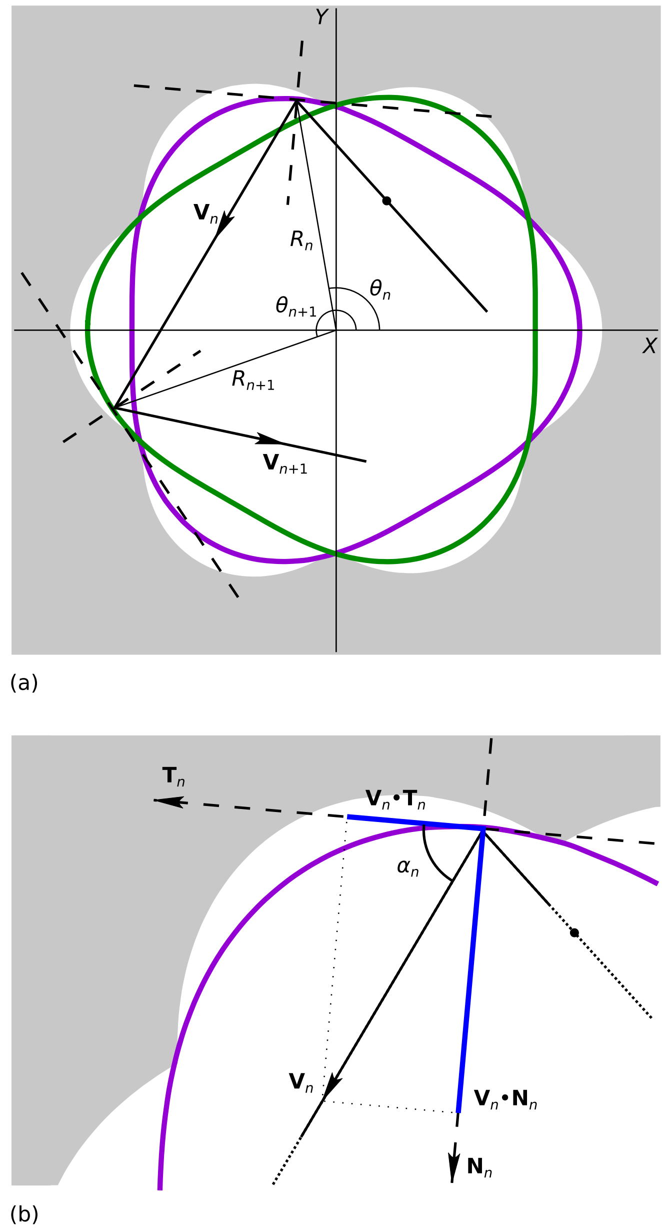

FIG. 1. (a) Piece of a particle's trajectory in the billiard under investigation. (b) Amplification of a portion on the top left of (a).

The particle's velocity has two components, a tangential and a normal. If the collisions of the particle with the boundary are inelastic, partial loss of energy is observed, affecting, according to the reflection law, only the normal component of the velocity. At the instant of collision, the reflection law is written as

$$\mathbf{V}'_{n+1} \cdot \mathbf{T}_{n+1} = \mathbf{V}'_n \cdot \mathbf{T}_{n+1}, \tag{4}$$

$$\mathbf{V}'_{n+1} \cdot \mathbf{N}_{n+1} = -\gamma \mathbf{V}'_n \cdot \mathbf{N}_{n+1}, \tag{5}$$

where $\gamma \in [0, 1]$ is the restitution coefficient. If $\gamma = 1$, the collisions are completely elastic, allowing the system to exhibit Fermi acceleration as the LRA conjecture states, whereas $\gamma < 1$ leads to a fractional energy loss of the particles. The term $\mathbf{V}'$ corresponds to the velocity of the particle in the noninertial reference frame of the boundary; the normal and tangent unit vectors are given, respectively, by

$$\mathbf{N}_{n+1} = -\sin(\phi_{n+1})\mathbf{i} + \cos(\phi_{n+1})\mathbf{j}, \tag{6}$$

$$\mathbf{T}_{n+1} = \cos(\phi_{n+1})\mathbf{i} + \sin(\phi_{n+1})\mathbf{j}. \tag{7}$$

After the $n + 1$ impact, the tangential and normal velocity components are given by

$$\mathbf{V}_{n+1} \cdot \mathbf{T}_{n+1} = \mathbf{V}_n \cdot \mathbf{T}_{n+1}, \tag{8}$$

$$\begin{aligned} &\mathbf{V}_{n+1} \cdot \mathbf{N}_{n+1} \\ &\quad = -\gamma \mathbf{V}_n \cdot \mathbf{N}_{n+1} + (1+\gamma)\mathbf{V}_b(t_{n+1} + Z(n)) \cdot \mathbf{N}_{n+1}, \end{aligned} \tag{9}$$

where $\mathbf{V}_b(t_{n+1} + Z(n))$ corresponds to the boundary velocity given by

$$\mathbf{V}_b = \left.\frac{dR}{dt}\right|_{t_{n+1}+Z(n)} [\cos(\theta_{n+1})\mathbf{i} + \sin(\theta_{n+1})\mathbf{j}]. \tag{10}$$

The term $Z(n)$ is a random number between 0 and 2π introduced to create a stochastic behavior in the movement of the oscillating boundary. The introduction guarantees that the $\alpha \times \theta$ plane is covered uniformly, i.e., the chaotic orbit can diffuse in all parts of the phase space. As a side remark, we mention that the stochastic oval billiard can be considered as a model for heat transfer of a gas [12], as a potential application.

Finally, the speed of the particle and the angle α at the collision $(n + 1)$ are given, respectively, by

$$V_{n+1} = \sqrt{(\mathbf{V}_{n+1} \cdot \mathbf{T}_{n+1})^2 + (\mathbf{V}_{n+1} \cdot \mathbf{N}_{n+1})^2}, \tag{11}$$

$$\alpha_{n+1} = \arctan\left[\frac{\mathbf{V}_{n+1} \cdot \mathbf{N}_{n+1}}{\mathbf{V}_{n+1} \cdot \mathbf{T}_{n+1}}\right]. \tag{12}$$

With the above equations, the description of the system is complete.

The dissipative oval billiard has a transition from limited for $\gamma \neq 1$ to unlimited energy growth for $\gamma = 1$ [4,34]. It has been shown that for restitution parameter values close to but different from one, the dissipation is sufficient to prevent the particle from showing FA. When γ is increased to reach the critical value, the system displays scale invariance accompanying the TLUG. Since our goal is to characterize the TLUG, we focus on the discussion of on finding the order parameter and its corresponding susceptibility.

III. THE TRANSITION FROM LIMITED TO UNLIMITED ENERGY GROWTH

Three parameters control the system: η, associated with the movement of the boundary, ε, related to the amplitude of the circle deformation, and γ, denoting the restitution parameter. For $\eta = 0$, the billiard is static, and the system is nonintegrable. Depending on ε and the initial conditions, chaotic components are observed in the phase space, and corresponding FA is expected to occur in the driven billiard. This holds for values of the parameter $\varepsilon \neq 0$ because the system turns into the circular billiard if $\varepsilon = 0$, whose static version is integrable. Therefore, for $\eta\varepsilon \neq 0$, the $\theta \times \alpha$ plane displays a chaotic sea, and chaotic diffusion is observed in the dynamics.

The natural observable along the chaotic dynamics to prove the existence of the diffusion is the square root of the averaged squared velocity, given by

$$V_{\mathrm{rms}} = \sqrt{\frac{1}{M}\sum_{i=1}^{M}\frac{1}{n}\sum_{j=1}^{n} V_{i,j}^2}, \tag{13}$$

where M corresponds to the number of initial conditions whereas n is the number of collisions of the particle with the boundary. As discussed in Ref. [34], the behavior of V_{rms} is described as follows and as shown in Fig. 2. For relatively low initial velocity, $V_0 \approx 0$, the curves of V_{rms} grow as $V_{\mathrm{rms}} \propto [n(\eta\varepsilon)^2]^\beta$ with $\beta \cong 1/2$ yielding the diffusion of particles in the velocity space to be equivalent to a normal diffusion. For large enough n, the curves bend towards a regime of saturation given by a constant plateau [12], marking a limitation for diffusion $V_{\mathrm{sat}} \propto (1-\gamma)^{\alpha_1}(\eta\varepsilon)^{\alpha_2}$ with $\alpha_1 = (-1/2), \alpha_2 = 1$. The changeover from growth to the saturation is written as $n_x \propto (1-\gamma)^{z_1}(\eta\varepsilon)^{z_2}$, $z_1 = -1$, and $z_2 = 0$. Using proper scaling, all curves shown in Fig. 2(a) fall onto each other in a single and universal plot confirming a scale invariance for the chaotic diffusion, as shown in Fig. 2(b). Similar values of ε and η whose product is the same as the ones used in Fig. 2 provide indistinguishable results if the following two parameter ranges are avoided: (1) $\varepsilon \approx 0$ or, similarly, extremely high values of η, in which case the billiard takes the shape similar to a circle, and (2) for very small values of η (i.e., $\eta \approx 0$), for which the billiard approaches the static regime.

The parameter controlling the criticality of the system is γ. For $\gamma = 1$, FA can be observed, whereas $\gamma < 1$ leads to the suppression of the energy gained by the particle. As a consequence, FA is no longer observed. This changeover is observed in both stochastic and periodically driven models. Moreover, as can be seen in Fig. 2, the root-mean-square velocity behaves very similarly in both cases, showing only a small deviation. In light of this fact, we now proceed to calculate a candidate for the order parameter for the transition. The order parameter goes continuously to zero for a second-order phase transition while its susceptibility diverges in the same limit. In previous works [12,35], a set of critical exponents was provided using a phenomenological approach and considering a set of scaling hypotheses allied with a homogeneous function. The plateau marking the saturation regime for the root mean square of the squared average velocity is given by $V_{\mathrm{rms,sat}} \propto (1-\gamma)^{-1/2}$, therefore diverging in the limit of $\gamma \to 1$. However, an observable defined as $\sigma = 1/V_{\mathrm{rms,sat}} \propto$

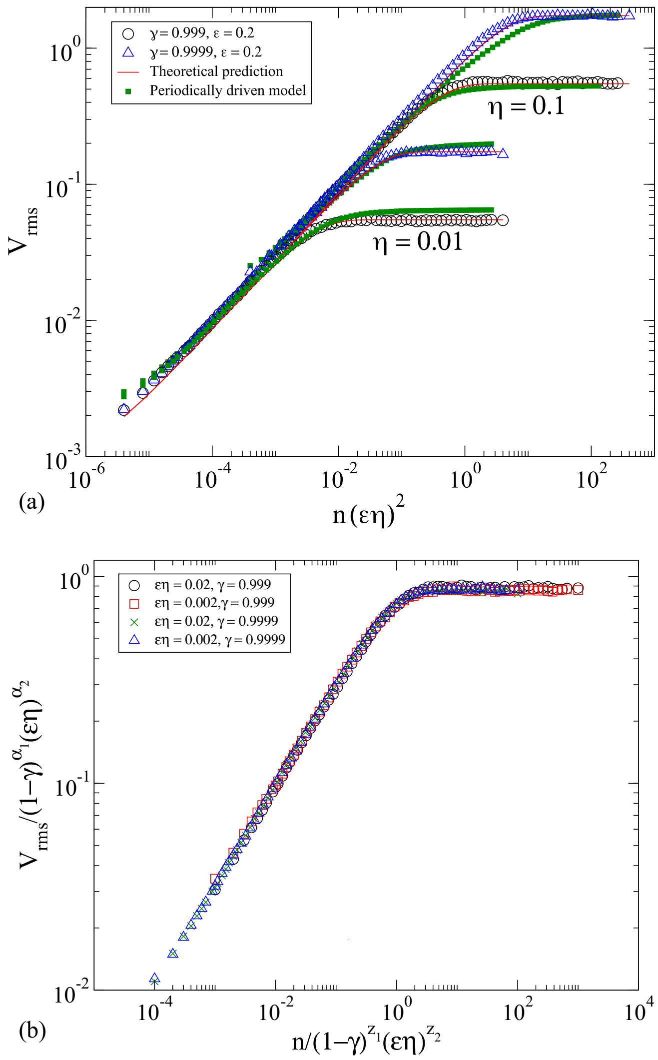

FIG. 2. (a) $V_{\rm rms}$ vs $n(\eta\varepsilon^2)$ for different values of γ close to the critical point, $\varepsilon = 0.2$ and two different values of η. The circles represent the numerical results for the stochastic model and the green squares for the periodically driven billiard, while the solid lines were obtained analytically. (b) Overlap of the $V_{\rm rms}$ curves after the following scaling transformations: (i) $V \to V/[(1-\gamma)^{\alpha_1}(\eta\varepsilon)^{\alpha_2}]$; (ii) $n \to n/[(1-\gamma)^{z_1}(\eta\varepsilon)^{z_2}]$.

$\sqrt{1-\gamma}$ is eligible as an order parameter. We note that our definition of this order parameter is to be understood as encapsulating the qualitative change of the energy growth while a vanishing value of σ indicates that the critical point $\gamma = 1$ is approached. Indeed, it goes continuously to zero in the limit $\gamma \to 1$. Its susceptibility, defined as $\chi = \frac{\partial\sigma}{\partial\gamma}$, diverges in the same limit.

Let us now discuss the results for the average squared velocity. For the stochastic model, in which we consider the random number Z in the argument of the velocity of the wall, the probability distribution for the velocity in the two-dimensional phase space α vs θ is uniform. It allows us to assume the statistical independence between the velocity and the dynamical variables θ and α. In this case, taking the average of the velocity given by Eq. (11) for the ranges $\alpha \in [0,\pi]$, $\theta \in [0,\pi]$, and $t \in [0, 2\pi]$ leads to

$$\bar{V}^2_{n+1} = \frac{\bar{V}^2_n}{2} + \frac{\gamma^2\bar{V}^2_n}{2} + \frac{(1+\gamma)^2\eta^2\varepsilon^2}{8}. \tag{14}$$

Although the random number Z becomes irrelevant when talking about $|\mathbf{V}_{n+1}|$ for the range $t \in [0, 2\pi]$, its addition to the argument of the velocity of the wall is necessary. The phase space α vs θ is uniform, which is a necessary condition to obtain $\bar{V}^2_{n+1}$. The average squared velocity can be obtained assuming that $\bar{V}^2_{n+1} - \bar{V}^2_n = \frac{\bar{V}^2_{n+1}-\bar{V}^2_n}{(n+1)-n} \cong \frac{d\bar{V}^2}{dn} = \frac{\bar{V}^2(\gamma^2-1)}{2} + \frac{(1+\gamma)^2\eta^2\varepsilon^2}{8}$, where the differential equation has the following solution,

$$\bar{V}^2(n) = \bar{V_0}^2 e^{\frac{(\gamma^2-1)}{2}n} + \frac{(1+\gamma)}{4(1-\gamma)}\eta^2\varepsilon^2\left[1 - e^{\frac{(\gamma^2-1)}{2}n}\right]. \tag{15}$$

To compare the analytical prediction with the simulations, we must average $\bar{V}^2$ over the orbit, which leads to

$$\begin{aligned}\langle\bar{V}^2(n)\rangle &= \frac{1}{n+1}\sum_{i=0}^{n}\bar{V}^2(i)\\ &= \frac{(1+\gamma)}{4(1-\gamma)}\eta^2\varepsilon^2\\ &\quad + \frac{1}{n+1}\left(\bar{V_0}^2 - \frac{(1+\gamma)}{4(4-\gamma)\eta^2\varepsilon^2}\right)\left[\frac{1-e^{\frac{(\gamma^2-1)(n+1)}{2}}}{1-e^{\frac{(\gamma^2-1)}{2}}}\right].\end{aligned} \tag{16}$$

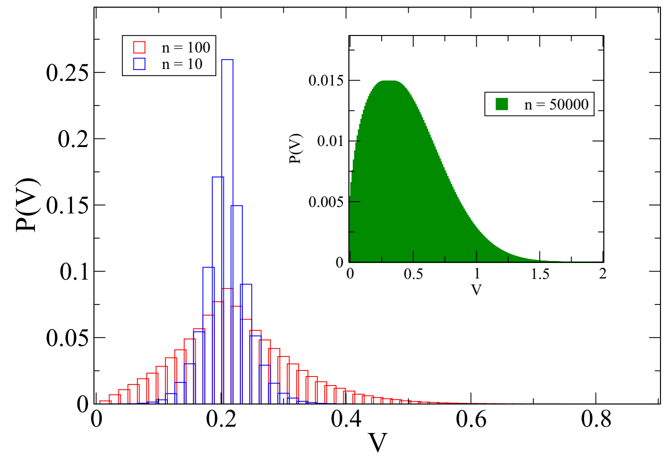

FIG. 3. Histogram of the normalized probability distribution for the velocity for an ensemble of 10^5 particles in the stochastic and dissipative oval billiard. The blue (dark gray) bars are obtained after ten collisions, while red bars (light gray) correspond to 100 collisions. The inset plot is obtained after 50 000 collisions. The initial velocity is $V_0 = 0.2$ and the control parameters are $\eta = 0.02$ and $\gamma = 0.999$ with $p = 2$.

Figure 3 shows the normalized probability distribution $P(V)$ for the three dynamical regimes: short, intermediate, and large time ranges. The parameters used are $\eta = 0.02$ and $\gamma = 0.999$. For larger times, a presumed Gaussian distribution flattens until the left-hand side of the curve reaches the lower velocity limit. The lower limit is given by the lowest velocity of the moving boundary. This change in probability behavior to a non-Gaussian distribution is similar to the one already observed in the Fermi-Ulam model [36,37].

Figure 2(a) shows the dependence of V_{rms} vs n for both stochastic and periodically driven models for different values of ε and η, as labeled in the figure. The range of parameters we are interested in is γ close to one, specifically $\gamma \in [0.999, 0.999\,95]$ and small $\varepsilon\eta \in [0.002, 0.02]$. The last interval was chosen to facilitate numerical simulations, but other positive values would give similar results. The symbols correspond to the numerical simulation obtained from the mapping iteration considering an ensemble of $M = 5 \times 10^3$ different initial conditions starting with the same initial velocity $V_0 = 0.001$. The solid lines denote the analytical results. As we can see, the agreement with the numerical curves is excellent.

Considering now the limit of $n \to \infty$, the saturation for the average velocity gives

$$V_{\mathrm{rms,sat}} = \sqrt{\frac{1+\gamma}{1-\gamma}\frac{\eta\varepsilon}{2}}. \tag{17}$$

As discussed earlier, the order parameter σ is then given by

$$\sigma = \frac{1}{V_{\mathrm{rms,sat}}} = \sqrt{\frac{1-\gamma}{1+\gamma}\frac{2}{\eta\varepsilon}}. \tag{18}$$

We notice σ depends on two sets of control parameters: (i) γ, which brings the criticality for the dynamics and makes $\sigma \to 0$ when $\gamma \to 1$, and (ii) $\eta\varepsilon$, which by the range of control parameters considered does not bring criticality to the dynamics.

Let us now determine the expression of the susceptibility χ, which gives information on how the order parameter responds to a variation of the control parameter γ responsible for the criticality. It is defined as

$$\chi = \frac{\partial\sigma}{\partial\gamma} = -\frac{2}{\eta\varepsilon(1+\gamma)^2}\sqrt{\frac{1+\gamma}{1-\gamma}}, \tag{19}$$

and it diverges in the limit $\gamma \to 1$.

Furthermore, it is worth noting that the mean velocity found in both the stochastic and periodically driven systems exhibits a strikingly similar behavior, as depicted in Fig. 2. As a result, we can employ $V_{\mathrm{rms,sat}}$ as an approximate order parameter to effectively describe the TLUG for both models. In this context, it is compelling to examine the fluctuations within the system prior to and on the critical point $\gamma = 1$. To accomplish this, we can assess the standard deviation ω of the velocity across M initial conditions:

$$\omega(\eta\varepsilon, n) = \frac{1}{M}\sum_{j=1}^{M}\sqrt{\overline{V^2}_j(\eta\varepsilon, n, V_0) - \overline{V}_j^2(\eta\varepsilon, n, V_0)}. \tag{20}$$

Figure 4(a) shows the behavior of the standard deviation ω for the dissipative and Fig. 4(b) for the nondissipative cases. Similar to V_{rms}, ω has a growth regime for low values of n and reaches a plateau after many collisions. Therefore, the fluctuations do not grow unbounded as they would for the nondissipative case. There is a rather limited range of fluctuations, which depends on the parameters η and ε. It indicates that the range of "interactions" during the TLUG is limited,

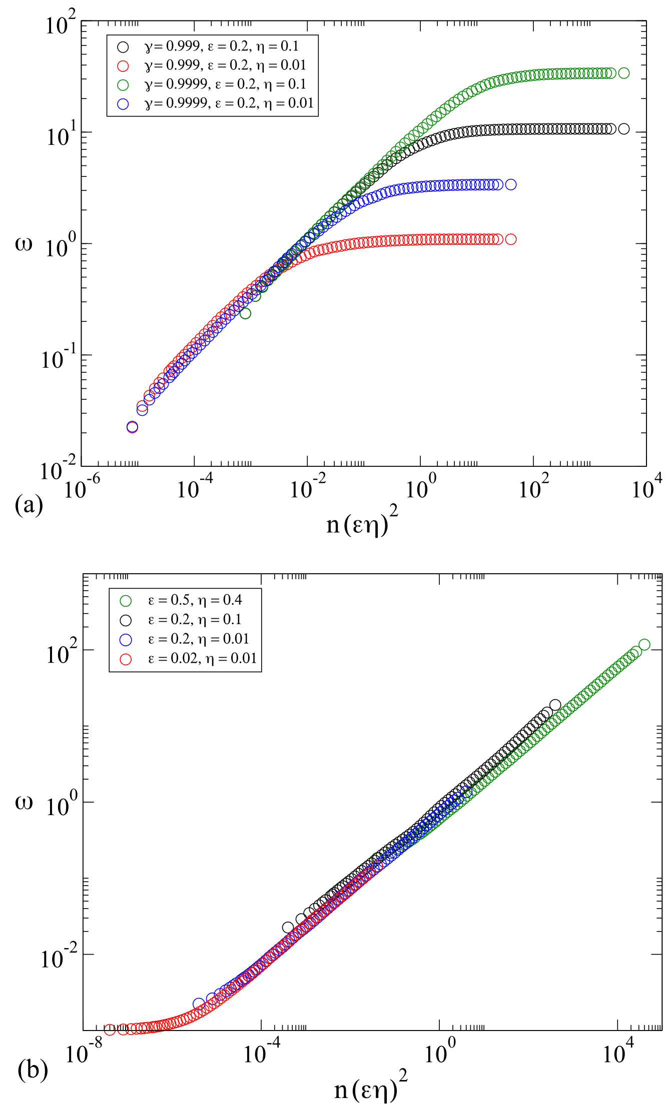

FIG. 4. Standard deviation of V_{rms} vs n for different values of the control parameters γ and $\varepsilon\eta$ for (a) the dissipative and (b) nondissipative cases. The horizontal axis is chosen to show the growth exponent is the same for all curves. Moreover, the standard deviation has the same critical exponents as the V_{rms} curves.

which is expected as the dissipation leads to a phase space contraction, suppressing the FA.

Moreover, to further assert the emergence of criticality when the critical point $\gamma = 1$ is reached, we calculate the mean cross-correlation $\overline{C}$ of M different trajectory velocities $V(n)$ in the phase space,

$$\overline{C} = \frac{1}{M}\sum_{i=1}^{M}\sum_{\substack{j=1\\ j\neq i}}^{M}\frac{\frac{1}{n}\sum_{k=1}^{n}[V_i(k) - \overline{V}_i][V_j(k) - \overline{V}_j]}{\sqrt{\left(\overline{V_i^2} - \overline{V}_i^2\right)\left(\overline{V_j^2} - \overline{V}_j^2\right)}}, \tag{21}$$

with the means of the velocities being taken over the number of collisions. Repeating this process for different values of γ in the range [0.995,1], we observe a sudden increase in the cross-correlation for $\gamma = 1$, as can be seen in Fig. 5. This result suggests the emergence of a collective behavior in the

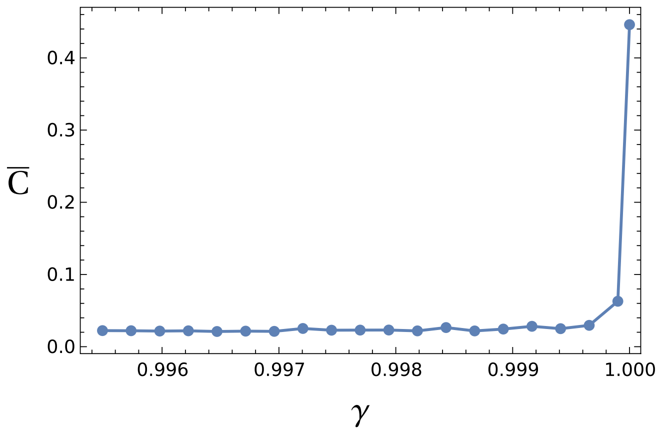

FIG. 5. Mean cross-correlation $\overline{C}$ for 20 different values of $\gamma \in [0.995, 1]$. Each data point represents the average of the cross-correlation between the $V(n)$ of 1000 initial conditions for a system with $\varepsilon = 0.1$ and $\eta = 0.1$. The average of the velocity is taken over 10^6 collision and each initial condition has initial velocity $V_0 = 0.001$.

velocity observable for different initial conditions when we approach the critical point.

The change in the velocity behavior can be easily traced for the general case by comparing the system's dynamics in two situations: when the collisions are elastic versus the collisions being inelastic.

Figure 6 illustrates the behavior of $V_{\rm rms}$ as a function of n for different values of $\varepsilon\eta$ considering elastic collisions, i.e., $\gamma = 1$. In this scenario, the system presents FA where, after a short number of collisions, the velocity increases monotonically with an exponent $\beta \approx 1/2$. However, for $\gamma < 1$, the dissipation implies an area contraction of the accessible phase space leading to the creation of attractors. Given they are far away from infinity, unlimited diffusion is prevented. Hence, for those values of γ, the system shows a saturation regime, as shown in Fig. 2, demonstrating that the unlimited energy growth has been suppressed.

Let us briefly discuss the elementary excitation responsible for the diffusion of the particles. Each particle of the ensemble's velocity changes after a collision with the boundary. In this context, the elementary excitation or the effect analogous to an elementary excitation occurs due to the product $\varepsilon\eta$, which is the maximal velocity of the billiard boundary. Therefore $\varepsilon\eta$ defines the elementary unit of the underlining random walk "motion" of the trajectories in the phase space. Indeed, if we take the limit of short times and small initial velocities, the diffusion of the velocity is given by $V \approx \frac{\eta\varepsilon}{2}\sqrt{n}$.

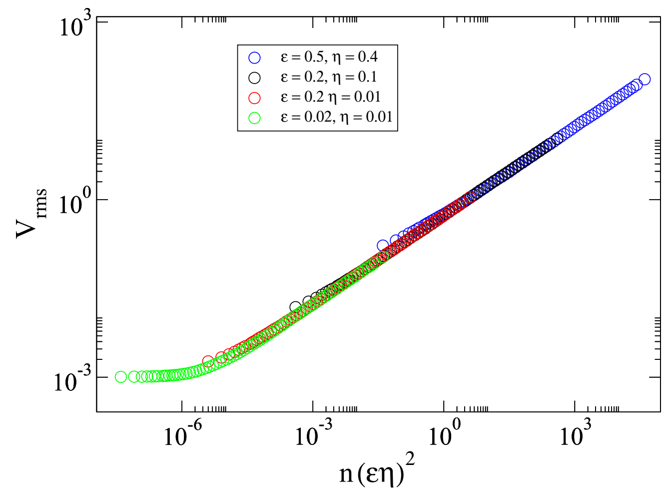

FIG. 6. $V_{\rm rms}$ vs n for the nondissipative oval billiard, i.e., $\gamma = 1$, for four different combinations of $\eta\epsilon$.

This shows that for a small n, the particle diffuses in the phase space analogously to a random walk with step size $\frac{\eta\varepsilon}{2}$.

IV. SUMMARY

We have analyzed Fermi acceleration in a driven and stochastified oval billiard with and without dissipation emphasizing its unlimited versus limited energy growth. Our focus was hereby on the analogy to a phase transition taking place from the nondissipative to the dissipative dynamics. The suppression of infinite diffusion in momentum space happens due to inelastic collisions leading the dynamics for a sufficiently long time to approach a saturation regime. We identified an order parameter that goes continuously to zero at the critical point and whose corresponding susceptibility diverges in the same limit. We argued that the found order parameter should be also applicable to the periodically driven billiard. The elementary excitation is given by the change of the velocity in an elementary collision and we suggest it depends on the product of the involved parameters of the driven oval billiard. Altogether this makes us conclude that the TLUG shares several features with a common phase transition of second order.

ACKNOWLEDGMENTS

F.A.O.S. acknowledges CAPES (No. 88887.670331/2022-00) for financial support. A.K.P.F. acknowledges FAPESP (2020/07219-1) for financial support. E.D.L. acknowledges support from Brazilian agencies CNPq (No. 301318/2019-0) and FAPESP (No. 2019/14038-6 and No. 2021/09519-5).

[1] N. S. Krylov, *Works on the Foundations of Statistical Physics* (Princeton University Press, Princeton, NJ, 1979).
[2] N. Chernov and R. Markarian, *Chaotic Billiards* (American Mathematical Society, Providence, RI, 2006), Vol. 127.
[3] A. Loskutov, A. B. Ryabov, and L. G. Akinshin, J. Exp. Theor. Phys. **89**, 966 (1999).
[4] A. Loskutov, A. B. Ryabov, and L. G. Akinshin, J. Phys. A: Math. Gen. **33**, 7973 (2000).
[5] A. K. Karlis, P. K. Papachristou, F. K. Diakonos, V. Constantoudis, and P. Schmelcher, Phys. Rev. E **76**, 016214 (2007).
[6] D. F. M. Oliveira and E. D. Leonel, Chaos **22**, 026123 (2012).

[7] C. P. Dettmann and O. Georgiou, Phys. Rev. E **83**, 036212 (2011).
[8] E. D. Leonel, D. F. M. Oliveira, and A. Loskutov, Chaos **19**, 033142 (2009).
[9] F. Lenz, F. K. Diakonos, and P. Schmelcher, Phys. Rev. Lett. **100**, 014103 (2008).
[10] F. Lenz, C. Petri, F. R. N. Koch, F. K. Diakonos, and P. Schmelcher, New J. Phys. **11**, 083035 (2009).
[11] E. D. Leonel and L. A. Bunimovich, Phys. Rev. Lett. **104**, 224101 (2010).
[12] E. D. Leonel, M. V. C. Galia, L. A. Barreiro, and D. F. M. Oliveira, Phys. Rev. E **94**, 062211 (2016).
[13] A. K. Karlis, F. K. Diakonos, and V. Constantoudis, Chaos **22**, 026120 (2012)
[14] V. Gelfreich, V. Rom-Kedar, and D. Turaev, Chaos **22**, 033116 (2012).
[15] F. Comets, S. Popov, G. M. Schütz, and M. Vachkovskaia, Arch. Ration. Mech. Anal. **191**, 497 (2009).
[16] T. Chumley, S. Cook, and R. Feres, Comput. Math. Appl. **65**, 1596 (2013).
[17] R. Feres and G. Yablonsky, Chem. Eng. Sci. **59**, 1541 (2004).
[18] S. Cook and R. Feres, Nonlinearity **25**, 2503 (2012).
[19] Z. H. Yakhini, Ph.D. thesis, Stanford University, 1997.
[20] D.-Q. Jiang, M. Qian, and M.-P. Qian, *Mathematical Theory of Nonequilibrium Steady States*, Lecture Notes in Mathematics Vol. 1833 (Springer, Berlin, 2004).
[21] D. Ruelle, J. Stat. Phys. **95**, 393 (1999).
[22] M. L. Kavvas, R. S. Govindaraju, and U. Lall, Chaos **25**, 075201 (2015).
[23] K. E. Chlouverakis and J. C. Scprott, Chaos **17**, 023110 (2007).
[24] G. M. Zaslavsky, M. Edelman, and B. A. Niayzov, Chaos **7**, 159 (1997).
[25] Y. Pesin, M. Shlesinger, Y. Sinai, and G. Zaslavsky, Chaos **7**, 1 (1997).
[26] M. J. Feigenbaum, J Stat. Phys. **19**, 25 (1978).
[27] E. Fontich and J. J. Sardanyés, J. Phys. A: Math. Theor. **41**, 015102 (2008).
[28] L. E. Reichl, *A Modern Course in Statistical Physics*, 2nd ed. (Wiley, 1998).
[29] A. L. Barabási and H. E. Stanley, *Fractal Concepts in Surface Growth* (Cambridge University Press, Cambridge, UK, 1985).
[30] J. Cardy, *Scaling and Renormalization in Statistical Physics* (Cambridge University Press, Cambridge, UK, 2003).
[31] L. P. Kadanoff, *Statistical Physics: Statics, Dynamics and Renormalization* (World Scientific, Singapore, 2000).
[32] E. D. Leonel, P. V. E. McClintock, and J. K. L. da Silva, Phys. Rev. Lett. **93**, 014101 (2004).
[33] D. G. Ladeira and J. K. L. da Silva, J. Phys. A: Math. Theor. **41**, 365101 (2008).
[34] D. F. M. Oliveira and E. D. Leonel, Physica A **389**, 1009 (2010).
[35] E. D. Leonel and C. P. Dettmann, Phys. Lett. A **376**, 1669 (2012).
[36] D. F. M. Oliveira, M. R. Silva, and E. D. Leonel, Physica A **436**, 909 (2015).
[37] E. D. Leonel, M. Yoshida, and J. A. Oliveira, Europhys. Lett. **131**, 20002 (2020).